12. Morimoto T, Miyoshi T, Matsuda S, Tano Y, Fujikado T, Fukuda Y. Transcorneal electrical stimulation rescues axotomized retinal ganglion cells by activating endogenous retinal IGF-1 systems. *Invest Ophthalmol Vis Sci.* 2005;46:2147-2155.
13. Sato T, Fujikado T, Morimoto T, Matsushita K, Harada T, Tano Y. Effect of electrical stimulation on IGF-1 transcription by L-type calcium channels in cultured retinal Müller cells. *Jpn J Ophthalmol.* 2008;52:217-223.
14. Miller RJ. Rocking and rolling with Ca2+ channels. *Trends Neurosci.* 2001;24:445-449.
15. Ou LC, Gean PW. Transcriptional regulation of brain-derived neurotrophic factor in the amygdala during consolidation of fear memory. *Mol Pharmacol.* 2007;72:350-358.
16. Sasaki M, Gonzalez-Zulueta M, Huang H, et al. Dynamic regulation of neuronal NO synthase transcription by calcium influx through a CREB family transcription factor-dependent mechanism. *Proc Natl Acad Sci USA.* 2000;97:8617-8622.
17. Ploski JE, Newton SS, Duman RS. Electroconvulsive seizure-induced gene expression profile of the hippocampus dentate gyrus granule cell layer. *J Neurochem.* 2006;99:1122-1132.
18. Follesa P, Biggio F, Gorini G, et al. Vagus nerve stimulation increases norepinephrine concentration and the gene expression of BDNF and bFGF in the rat brain. *Brain Res.* 2007;1179:28-34.
19. Geremia NM, Gordon T, Brushart TM, Al-Majed AA, Verge VMK. Electrical stimulation promotes sensory neuron regeneration and growth-associated gene expression. *Exp Neurol.* 2007;205:347-359.
20. Brosenitsch TA, Katz DM. Physiological patterns of electrical stimulation can induce neuronal gene expression by activating N-type calcium channels. *J Neurosci.* 2001;21:2571-2579.
21. Zhao R, Liu L, Rittenhouse AR. Ca2+ influx through both L- and N-type Ca2+ channels increases c-fos expression by electrical stimulation of sympathetic neurons. *Eur J Neurosci.* 2007;25:1127-1135.
22. Roque RS, Caldwell RB, Behzadian MA. Cultured Müller cells have high levels of epidermal growth factor receptors. *Invest Ophthalmol Vis Sci.* 1992;33:2587-2595.
23. Johnson MR, Wang K, Smith JB, Heslin MJ, Diasio RB. Quantitation of dihydropyrimidine dehydrogenase expression by real-time reverse transcription polymerase chain reaction. *Anal Biochem.* 2000;278:175-184.
24. Bourinet E, Mangoni ME, Nargeot J. Dissecting the functional role of different isoforms of the L-type Ca2+ channel. *J Clin Invest.* 2004;113:1382-1384.
25. Barde YA, Edgar D, Thoenen H. Purification of a new neurotrophic factor from mammalian brain. *EMBO J.* 1982;1:549-553.
26. Canals JM, Checa N, Marco S, et al. Expression of brain-derived neurotrophic factor in cortical neurons is regulated by striatal target area. *J Neurosci.* 2001;21:117-124.
27. Bifrare YD, Kummer J, Joss P, Tauber MG, Leib SL. Brain-derived neurotrophic factor protects against multiple forms of brain injury in bacterial meningitis. *J Infect Dis.* 2005;191:40-45.
28. Almeida RD, Manadas BJ, Melo CV, et al. Neuroprotection by BDNF against glutamate-induced apoptotic cell death is mediated by ERK and PI3-kinase pathways. *Cell Death Differ.* 2005;12:1329-1343.
29. Klocker N, Cellerino A, Bahr M. Free radical scavenging and inhibition of nitric oxide synthase potentiates the neurotrophic effects of brain-derived neurotrophic factor on axotomized retinal ganglion cells in vivo. *J Neurosci.* 1998;18:1038-1046.
30. Klocker N, Kermer P, Weishaupt JH, Labes M, Ankerhold R, Bahr M. Brain-derived neurotrophic factor-mediated neuroprotection of adult rat retinal ganglion cells in vivo does not exclusively depend on phosphatidyl-inositol-3′-kinase/protein kinase B signaling. *J Neurosci.* 2000;20:6962-6967.
31. Ko ML, Hu DN, Ritch R, Sharma SC, Chen CF. Patterns of retinal ganglion cell survival after brain-derived neurotrophic factor administration in hypertensive eyes of rats. *Neurosci Lett.* 2001;305:139-142.
32. Chen H, Weber AJ. BDNF enhances retinal ganglion cell survival in cats with optic nerve damage. *Invest Ophthalmol Vis Sci.* 2001;42:966-974.
33. Nakazawa T, Tamai M, Mori N. Brain-derived neurotrophic factor prevents axotomized retinal ganglion cell death through MAPK and PI3K signaling pathways. *Invest Ophthalmol Vis Sci.* 2002;43:3319-3326.
34. Paskowitz DM, Donohue-Rolfe KM, Yang H, et al. Neurotrophic factors minimize the retinal toxicity of verteporfin photodynamic therapy. *Invest Ophthalmol Vis Sci.* 2007;48:430-437.
35. Fujikado T, Morimoto T, Matsushita K, Shimojo H, Okawa Y, Tano Y. Effect of transcorneal electrical stimulation in patients with nonarteritic ischemic optic neuropathy or traumatic optic neuropathy. *Jpn J Ophthalmol.* 2006;50:266-273.
36. Oku H, Ikeda T, Honma Y, et al. Gene expression of neurotrophins and their high-affinity Trk receptors in cultured human Müller cells. *Ophthalmic Res.* 2002;34:38-42.

Adaptive Optics Fundus Camera to Examine Localized Changes in the Photoreceptor Layer of the Fovea

Yoshiyuki Kitaguchi, MD,[1] Takashi Fujikado, MD,[1] Kenichiro Bessho, MD,[1] Hirokazu Sakaguchi, MD,[2] Fumi Gomi, MD,[2] Tatsuo Yamaguchi, MS,[3] Naoki Nakazawa, BE,[3] Toshifumi Mihashi, PhD,[3] Yasuo Tano, MD[2]

Purpose: To examine highly localized photoreceptor disruptions in the fovea by a high-resolution adaptive optics (AO) fundus camera combined with Fourier-domain optical coherence tomography (FD OCT).

Design: Observational case series.

Participants: Three eyes of 3 patients who showed dark foveal spots by slit-lamp biomicroscopy.

Methods: Three patients who reported metamorphopsia but showed no changes in the retina in conventional fundus photographs were examined. High-resolution retinal images were obtained with the AO fundus camera and by FD OCT. The images were compared with the findings obtained by standard clinical tests, including Amsler charts and fluorescein angiography (FA).

Main Outcome Measures: Quantitative measurements of the area of photoreceptor disruption.

Results: Slit-lamp biomicroscopy revealed an irregularly shaped dark spot in the fovea centralis but no changes in FA in the 3 cases. The photoreceptor mosaic was absent in a highly localized area of the fovea in the images obtained by the AO fundus camera, and the photoreceptor outer segment was absent or disturbed at the corresponding area by FD OCT in all 3 cases. The horizontal and vertical sizes of the area of disturbance of the photoreceptor mosaic in the AO images in the 3 eyes were 400×200 μm, 300×120 μm, and 300×200 μm. These sizes were comparable to the photoreceptor outer segment disturbances in the OCT images which were 330×150 μm, 280×100 μm, 200×150 μm, respectively.

Conclusions: Localized OS disturbances were able to be detected in eyes with a dark foveal spot by AO fundus camera 2-dimensionally and by FD OCT axially. The good correspondence of the sizes of the area of photoreceptor disturbances obtained by AO images to those by FD OCT images indicate that the AO images can be used to evaluate and follow the 2-dimensional area of focal changes of the photoreceptors in the fovea quantitatively.

Financial Disclosure(s): Proprietary or commercial disclosure may be found after the references.
Ophthalmology 2008;115:1771–1777 © 2008 by the American Academy of Ophthalmology.

With current advanced retinal imaging instruments, small focal changes of the retina can be detected and measured more accurately. These findings can help in determining the cause of unexplained visual symptoms and visual loss. For example, the retina of patients at the early phase of macular dystrophy appears ophthalmoscopically normal.[1–6] However, examination of optical coherence tomography (OCT) images showed that the retina was thinner at the macular area and that the decrease in thickness was correlated with the reduced visual acuity.[4] With additional improvements in the axial resolution by ultra–high-resolution OCT, several studies have shown a good correlation between the disruption of the photoreceptor inner segment/outer segment (IS/OS) junction and the decrease in visual acuity.[7–10] Ultra–high-resolution OCT, or Fourier-domain (FD) OCT, has an axial resolution of approximately 3 to 5 μm,[9–12] which is significantly better than the axial resolution of approximately 10 μm with the standard OCT. This increased resolution results in better delineation of the retinal architecture and helps in identifying pathologic changes in the microstructure of the retina, especially the photoreceptor layer.[9–11]

A disturbance of IS/OS junction has been reported in cases of postoperative retinal detachment, central serous chorioretinopathy, and retinal dystrophy.[7,8,10,11,13,14] Some studies have found a good correlation between the disturbance of IS/OS junction and the visual acuity.[4,7,10,11]

One problem with conventional OCT is its low transverse resolution. Generally, the transverse resolution of OCT is on the order of 20 μm, which exceeds the cone mosaic spacing of 5 to 10 μm. Two reasons for this limitation are the ocular aberrations and saccadic eye movements. The A-scan technologies adopted in OCT are not suited for obtaining transverse information in both the x- and y-directions in a short acquisition time, and obtaining motion-artifact–free 2-dimesional transverse images of the cone mosaic is not possible.[16]

Adaptive optic (AO) systems seem to be well suited to overcome these problems. An AO system consists of a wavefront sensor to measure ocular aberrations and a de-

ISSN 0161-6420/08/$–see front matter
doi:10.1016/j.ophtha.2008.03.026

formable mirror to compensate for these aberrations. Correcting the ocular aberrations with the AO system can improve the transverse resolution to less than 2 μm, which is necessary to image individual photoreceptors in the living retina.[16–20] Because transverse 2-dimensional images of the retina can be obtained with the AO system, precise detection and measurements of small lesions can be made. Thus, the AO images of patients with cone dystrophy have been reported to have a patchy configuration because of photoreceptor dropout.[21–23] The limitation of the AO system is its low axial resolution. The axial resolution of AO system is approximately 100 μm, even when it is coupled with a scanning laser ophthalmoscope.[19] It is even greater with conventional flood-illumination fundus photography.

Because of the complementary aspects of FD OCT and AO, that is, high axial resolution with FD OCT and high transverse resolution with the AO system, it theoretically would be valuable to combine both instruments to evaluate small focal photoreceptor disruptions. However, the authors have not found a publication that used both systems to compare the images obtained with FD OCT and those obtained with the AO system. The authors have developed a compact, clinically friendly AO fundus camera using a liquid crystal phase modulator. With this instrument, they have been able to show the increased cone spacing in myopic eyes.[24] The purpose of this study was to determine the cause of dark spots in the fovea of 3 patients with metamorphopsia. In all 3 patients, the fundus appeared ophthalmoscopically normal and the photographs obtained by conventional fundus photography also demonstrated normal results. These retinas were examined with their custom-built AO fundus camera, and the images were compared with the OCT images.

Patients and Methods

Patients

Three consecutive patients who reported metamorphopsia but whose photographs of the ocular fundus by standard fundus photography demonstrated normal results were studied. All patients had visited Osaka University Hospital between January and June 2006. The research protocol was approved by the Institutional Review Board of the Osaka University Medical School, and the procedures conformed to the tenets of the Declaration of Helsinki. After the nature and possible consequences of the study were explained, written informed consent was obtained from all patients.

Procedures

All patients underwent a comprehensive ophthalmologic examination, including the measurement of best-corrected visual acuity (BCVA), Amsler chart, fundus photography, and slit-lamp biomicroscopy of the fundus. They also underwent examinations by FD OCT (RTVue-100; Optovue, Inc., Fremont, CA) and a custom-built AO fundus camera.[24] All 3 patients also underwent fluorescein angiography (FA) and indocyanine green angiography (ICGA).

Adaptive Optic Fundus Camera

A detailed description of the custom-built AO fundus camera has been published.[24] The principle of this flood illumination AO fundus camera was similar to that reported by Roorda and Williams.[17] Briefly, the main components of the camera were a nematic liquid crystal phase modulator (X8267–12; Hamamatsu Photonics, Hamamatsu, Japan), a Hartmann-Shack wavefront sensor (28×28 lenslets; specially made by Topcon, Co., Tokyo, Japan), and a scientific charge-coupled device digital camera (C9100–02; Hamamatsu Photonics).

The wavefront sensor measured the ocular wavefront up to the eighth Zernike order, and the phase modulator compensated for the measured wavefront aberrations. The system also is equipped with coaxial, 8-degree–wide viewing optics to identify the location and orientation of the highly magnified retinal images being observed.

Topical tropicamide (0.5%) and phenylephrine (0.5%) were used to dilate the pupil and to paralyze the ciliary muscle. The retina was illuminated with a 2-ms flash (635-nm wavelength) from a xenon arc lamp, and a retinal image was obtained with a 6-mm–diameter exit pupil. The patient was instructed to fixate a designated location on a target. Frame averaging was performed using custom software (Topcon) to improve the quality of the image. Overlapping images were merged using Photoshop (Adobe Systems, Inc., San Jose, CA). To identify the fovea, a montage of the AO images was made and superimposed on the fundus photographs and the fundus projection of OCT images.

Case Reports

Patient 1. A 39-year-old man reported metamorphopsia in his left eye which began 3 months earlier. His BCVA was 20/15 in both eyes. Ophthalmoscopy showed that the ocular fundus appeared normal in both eyes (Fig 1A). Slit-lamp biomicroscopy showed an irregularly shaped dark spot in the fovea centralis of the left eye. Amsler chart examination showed a localized area of metamorphopsia just below the fixation point.

Fourier-domain OCT demonstrated a disturbance of the IS/OS junction and OS layer (between second and third line of FD OCT) of approximately 330 μm on the horizontal scan and 150 μm on the vertical scan. The external limiting membrane layer was intact (Fig 1B,C).

The AO image showed a dark area, that is, an absence of the cone mosaic, at the fovea just above the fixation point. The shape of dark area was geographic, and the size was approximately 350 μm horizontally and 160 μm vertically (Fig 1D–F).

Patient 2. A 39-year-old man reported blurred vision and metamorphopsia in his right eye of 2 years' duration. His BCVA was 20/60 in the right eye and 20/20 in the left eye. He had been diagnosed with keratoconus in his right eye, but his vision did not improve after wearing a hard contact lens.

The ocular fundus appeared normal in fundus photographs (Fig 2A). Slit-lamp biomicroscopy showed an abnormal reflex in the macula and an irregularly shaped dark spot in the fovea centralis of the right eye. Amsler chart examination showed a central scotoma. Fluorescein angiography and ICGA did not show any abnormal findings (Fig 2B).

Fourier-domain OCT demonstrated a defect in the OS layer in the fovea that was located just under the IS/OS layer. The size of the defect was 280 μm on the horizontal scan and 100 μm on the vertical scan. The IS/OS junction was preserved but the intensity was slightly lower. The external limiting membrane and the RPE layers appeared to be normal (Fig 2C,D).

The AO image indicated a disappearance of the cone mosaic at the fovea. The dark area was oval, and the size was 300 μm horizontally and 120 μm vertically (Fig 2E–G).

Patient 3. A 62-year-old man reported metamorphopsia in his left eye of 6 months' duration. His BCVA was 20/200 in the right eye and 20/22 in the left eye. No abnormality was found in the ocular fundus in the conventional fundus photographs (Fig 3A). Slit-lamp biomicroscopy showed an irregularly shaped dark spot in the fovea centralis of the left eye. Amsler chart examination indicated a localized area of metamorphopsia just below the fixation point. The FA and ICGA results were normal (Fig 3B).

Fourier-domain OCT demonstrated an elevation of the external limiting membrane. The photoreceptor OS and IS/OS junction were not detected over an area of 200 μm on the horizontal scan and 150 μm on the vertical scan (Fig 3C,D).

The AO image demonstrated the disappearance of the cone mosaic at the foveal zone. At the fovea centralis, a relatively high reflective area without cone mosaic was observed. The area of the absence of foveal cones was approximately 300 μm horizontally and 200 μm vertically (Fig 3E,F).

Results

All 3 patients had metamorphopsia unilaterally, and the BCVA ranged 20/200 to 20/15 in the affected eye. The Amsler chart examination showed localized metamorphopsia in 2 eyes and a central scotoma in 1 eye. The ocular fundus appeared to be normal in standard fundus photographs, but slit-lamp biomicroscopy revealed an irregularly shaped dark spot in the fovea centralis in the 3 cases. Fluorescein angiography and ICGA did not show any abnormal findings in any cases.

Fourier-domain OCT demonstrated an absence of the OS and IS/OS junction of the photoreceptors in 1 case and an absence or disturbance of the OS but preservation of the IS/OS junction in 2 cases. The AO images indicated the absence of the cone mosaic in the foveal zone in all 3 cases. The horizontal and vertical sizes of the area of the absence of the photoreceptor mosaic in the AO images in the 3 eyes (400×200 μm, 300×120 μm, and 300×200 μm) were comparable with the sizes of the photoreceptor OS disturbances in the OCT images (330×150 μm, 280×100 μm, 200×150 μm, respectively).

Discussion

This study examined the FD OCT and AO images in patients who showed localized disturbances in the photoreceptor layer. To the best of the authors' knowledge, this is the first study that compares the FD OCT and AO images in the same patient. A localized disappearance of the photoreceptor mosaic was observed in the photographs of the fovea obtained by the AO fundus camera in all 3 cases. The horizontal and vertical sizes of the area of the loss of the photoreceptor mosaic in the AO images were comparable with the area of the OS disturbance in the OCT images. In patient 3, the IS/OS junction and OS were also not detected, but in patients 1 and 2, the IS/OS line was preserved, although the intensity was slightly lower than normal. These results suggested that the dark area seen by slit-lamp biomicroscopy corresponded with an absence of the photoreceptor mosaic in the AO images and with the disturbed photoreceptor OS in the OCT images.

The origin of the high reflectance cone mosaic in the AO fundus camera is reported to be from both the IS/OS junction and the OS in the normal retina.[15] However, based on the results from patient 1, a possibility exists that the OS is more involved in the reflectance of photoreceptor mosaic than the IS/OS junction in the AO images. This hypothesis corresponds with the results of a recent report using AO OCT, in which the cone mosaic is observed clearly at the level of Verhoeff's membrane (the third blight line of FD OCT), where the tip of the cone photoreceptor OS is enveloped by microvilli.[25]

In patients with a macular hole, metamorphopsia is a frequently reported symptom. In the early stage of macular hole, morphologic changes are observed not only in the photoreceptor layer, but also in the inner retinal layers because of the tangential traction on the retinal surface. All of the patients reported metamorphopsia, but the lesion was confined to only the photoreceptor layer and was in a very restricted area in the fovea.

Recently, a new clinical entity termed *foveal spot* or *macular microhole* has been proposed.[26,27] In this lesion, the patient has a mildly reduced visual acuity, a central scotoma, and metamorphopsia, and ophthalmoscopy shows a foveal defect with a red appearance and well-defined margins. The size of the lesion is approximately 100 μm and seems to be intraretinal. Conventional OCT3 images (Stratus model 3000; Carl Zeiss Meditec, Humphrey Division, Dublin, CA) show an abnormality of the outer retina, a defect of retinal pigment epithelium, or both.[27] All 3 of the eyes had an apparently normal ocular fundus by conventional fundus photography, but slit-lamp biomicroscopy showed an irregularly shaped dark spot in the fovea centralis. Thus, the 3 eyes may be included in the category of macular microhole or foveal spot. The decrease in the visual acuity or an increase in the area of metamorphopsia should be reflected in the size of the dark area in AO fundus image, and thus may be helpful to evaluate the progression of a disease quantitatively.

The limitation of this study is that the fovea could not be resolved accurately with the AO system. The AO system allows a transverse resolution of 2 μm, but the photoreceptors in the fovea are smaller than the resolution limit.[16–20] Because of this, it is difficult to identify the individual cones in the fovea centralis in the AO images. However, because the dark area is not observed in the central fovea in normal eyes, the dark area at or around the central fovea can be assumed to be the area of photoreceptor loss or disruption.

In conclusion, the AO fundus camera can acquire 2-dimensional images of the retina with a resolution of approximately 2 μm. This resolution allows the detection of highly localized disturbances of the photoreceptor cells that can correlate with the high-resolution images obtained by FD OCT. Combining the AO fundus camera and FD OCT images can be valuable to assess photoreceptor disruptions, especially in eyes with a small focal foveal lesion. The findings in these 3 patients indicate that patients reporting metamorphopsia may have a localized disruption the of photoreceptor cells in the fovea.

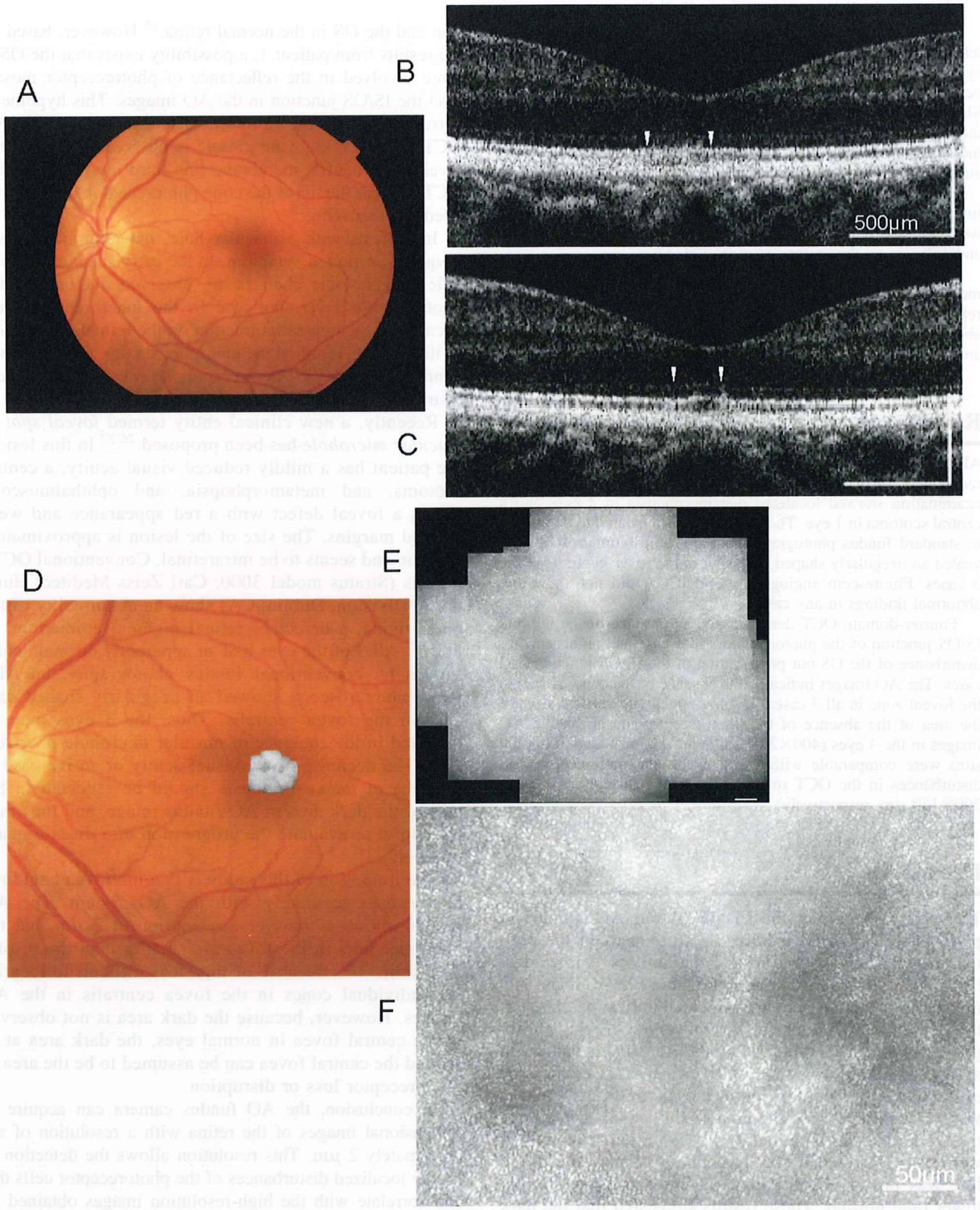

Figure 1. Images from the left eye of patient 1, who sought treatment for metamorphopsia. **A**, Fundus photograph showing normal appearance. **B**, Fourier-domain optical coherence tomography image (5-mm horizontal scan) demonstrating the disturbance of the inner segment/outer segment (IS/OS) junction and outer segment (OS) layer (between the second and third lines) for approximately 330 μm. **C**, Fourier-domain optical coherence tomography vertical scan showing the disturbance of the IS/OS junction and OS layer for approximately 150 μm. The arrowhead in **B** and **C** point to the area of IS/OS and OS disturbances. The horizontal bars in **B** and **C** represent 500 μm. **D**, Montage of adaptive optics (AO) image superimposed on the fundus photograph. **E**, Montage of adaptive optics image (low magnification). **F**, Magnified AO image of the fovea showing a dark area (disappearance of cone mosaic) at the fovea just above the fixation point. The shape of dark area was geographic and the size was approximately 350 μm horizontally and 180 μm vertically. The horizontal bars in **E** and **F** represent 50 μm.

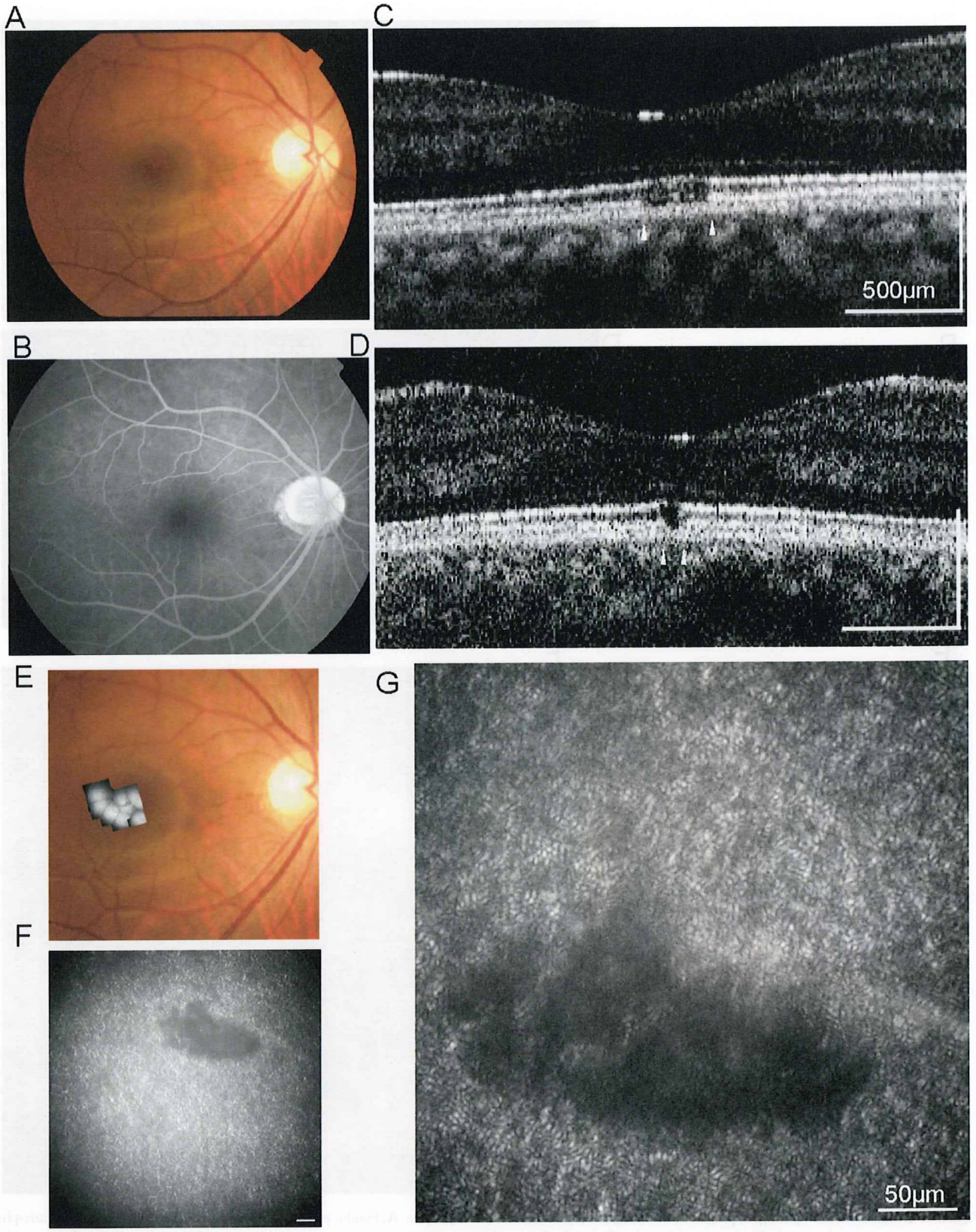

Figure 2. Images from the right eye of patient 2, who sought treatment for metamorphopsia. **A**, Fundus photograph showing that the retina appears to be normal. **B**, Early-phase fluorescein angiography image showing normal results. **C** and **D**, Fourier-domain optical coherence tomography images demonstrating a defect of outer segment (OS) layer in the fovea that was located just beneath the inner segment/OS junction. The size of the defect was (**C**) 280 μm on the horizontal scan and (**D**) 100 μm on the vertical scan. The IS/OS line was preserved but the intensity was slightly low. The arrowhead in **C** and **D** points to the area of OS defect. The horizontal bars in **C** and **D** represent 500 μm, and the vertical bars represent 200 μm. **E**, Montage of adaptive optics (AO) image superimposed on the fundus photograph. **F**, adaptive optics image (low magnification). **G**, Magnified AO image of the fovea showing a dark oval-shaped area (disappearance of cone mosaic) with a size of 300 μm horizontally and 120 μm vertically. The horizontal bars in **F** and **G** represent 50 μm.

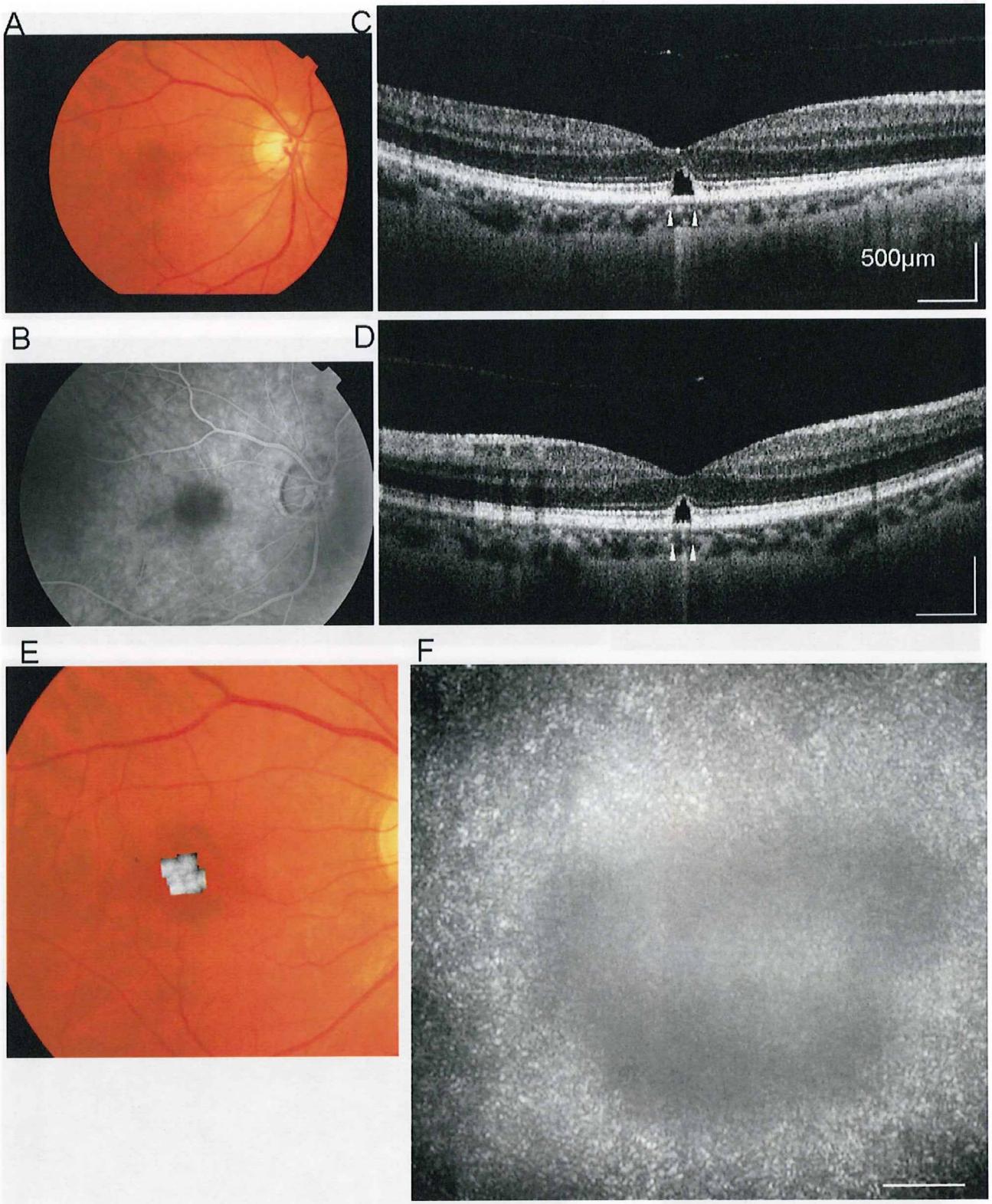

Figure 3. Images from the right eye of patient 3, who sought treatment for metamorphopsia. **A**, Fundus photograph showing normal appearance. **B**, Early-phase of fluorescein angiography image showing normal results. **C** and **D**, Fourier-domain optical coherence tomography images demonstrating the elevation of the external limiting membrane. Photoreceptor outer segment (OS) and inner segment/OS junction are not present in an area of (**C**) 200 μm on the horizontal scan and (**D**) 150 μm on the vertical scan. The arrowhead in **C** and **D** indicates the area of OS defect. The horizontal bars in **C** and **D** represent 500 μm, and the vertical bars represent 200 μm. **E**, Montage of adaptive optics (AO) image superimposed on the fundus photograph. **F**, Magnified image of AO image in the fovea demonstrating a dark oval-shaped area (disappearance of cone mosaic) with a size of 300 μm horizontally and 200 μm vertically. At the fovea centralis, a slightly high reflective area without cone mosaic was observed. The horizontal bars in **F** represent 50 μm.

References

1. Brockhurst RJ, Sandberg MA. Optical coherence tomography findings in occult macular dystrophy. Am J Ophthalmol 2007; 143:516–8.
2. Kondo M, Ito Y, Ueno S, et al. Foveal thickness in occult macular dystrophy. Am J Ophthalmol 2003;135:725–8.
3. Benhamou N, Souied EH, Zolf R, et al. Adult-onset foveomacular vitelliform dystrophy: a study by optical coherence tomography. Am J Ophthalmol 2003;135:362–7.
4. Sandberg MA, Brockhurst RJ, Gaudio AR, Berson EL. The association between visual acuity and central retinal thickness in retinitis pigmentosa. Invest Ophthalmol Vis Sci 2005;46: 3349–54.
5. Samsel A, Drobecka-Brydak E, Godowska-Brydak E, et al. Optical coherence tomography in Stargardt's dystrophy [in Polish]. Klin Oczna 2005;107:668–71.
6. Miyake Y, Horiguchi M, Tomita N, et al. Occult macular dystrophy. Am J Ophthalmol 1996;122:644–53.
7. Ergun E, Hermann B, Wirtitsch M, et al. Assessment of central visual function in Stargardt's disease/fundus flavimaculatus with ultrahigh-resolution optical coherence tomography. Invest Ophthalmol Vis Sci 2005;46:310–6.
8. Wirtitsch E, Ergun B, Hermann A, et al. Ultrahigh resolution optical coherence tomography in macular dystrophy. Am J Ophthalmol 2005;140:976–83.
9. Drexler W, Sattmann H, Hermann B, et al. Enhanced visualization of macular pathology with the use of ultrahigh-resolution optical coherence tomography. Arch Ophthalmol 2003;121:695–706.
10. Ojima Y, Hangai M, Sasahara M, et al. Three-dimensional imaging of the foveal photoreceptor layer in central serous chorioretinopathy using high-speed optical coherence tomography. Ophthalmology 2007;114:2197–207.
11. Schocket LS, Witkin AJ, Fujimoro JG, et al. Ultrahigh-resolution optical coherence tomography in patients with decreased visual acuity after retinal detachment repair. Ophthalmology 2006;113:666–72.
12. Alam S, Zawadski RJ, Choi S, et al. Clinical application of rapid serial Fourier-domain optical coherence tomography for macular imaging. Ophthalmology 2006;113:1425–31.
13. Piccolino FC, de la Longrais RR, Ravera G, et al. The foveal photoreceptor layer and visual acuity loss in central serous chorioretinopathy. Am J Ophthalmol 2005;139:87–99.
14. Iida T, Hagimura N, Sato T, Kishi S. Evaluation of central serous chorioretinopathy with optical coherence tomography. Am J Ophthalmol 2000;129:16–20.
15. Pircher M, Baumann B, Gotzinger E, Hitzenberger CK. Retinal cone mosaic imaged with transverse scanning optical coherence tomography. Optics Lett 2006;15:1821–3.
16. Liang J, Williams DR, Miller DT. Supernormal vision and high-resolution retinal imaging through adaptive optics. J Opt Soc Am A Opt Image Sci Vis 1997;14:2884–92.
17. Roorda A, Williams DR. The arrangement of the three cone classes in the living human eye. Nature 1999;397:520–2.
18. Roorda A, Williams DR. Optical fiber properties of individual human cones. J Vis 2002;2:404–12.
19. Roorda A, Romero-Borja F, Donnelly W III, et al. Adaptive optics scanning laser ophthalmoscopy. Opt Express [serial online] 2002;10:405–12. Available at: http://www.opticsexpress.org/abstract.cfm?id=68843. Accessed March 11, 2008.
20. Pallikaris A, Williams DR, Hofer H. The reflectance of single cones in the living human eye. Invest Ophthalmol Vis Sci 2003;44:4580–92.
21. Wolfing JI, Chung M, Carroll J, et al. High-resolution retinal imaging of cone-rod dystrophy. Ophthalmology 2006;113: 1014–9.
22. Choi SS, Double N, Hardy JL, et al. In vivo imaging of the photoreceptor mosaic in retinal dystrophies and correlations with visual function. Invest Ophthalmol Vis Sci 2006;47: 2080–92.
23. Duncan JL, Zhang Y, Gandhi J, et al. High-resolution imaging with adaptive optics in patients with inherited retinal degeneration. Invest Ophthalmol Vis Sci 2007;48:3283–91.
24. Kitaguchi Y, Bessho K, Yamaguchi T, et al. In vivo measurements of cone photoreceptor spacing in myopic eyes from images obtained by an adaptive optics fundus camera. Jpn J Ophthalmol 2007;51:456–61.
25. Zawadzki RJ, Choi SS, Jones SM, et al. Adaptive optics-optical coherence tomography: optimizing visualization of microscopic retinal structures in three dimensions. J Opt Soc Am A Opt Image Sci Vis 2007;24:1373–83.
26. Douglas RS, Duncan J, Brucker A, et al. Foveal spot: a report of thirteen patients. Retina 2003;23:348–53.
27. Zambarakji HJ, Schlottmann P, Tanner V, et al. Macular microholes: pathogenesis and natural history. Br J Ophthalmol 2005;89:189–93.

Footnotes and Financial Disclosures

Originally received: November 25, 2007.
Final revision: March 16, 2008.
Accepted: March 25, 2008.
Available online: May 16, 2008. Manuscript no. 2007-1518.

[1] Department of Applied Visual Science, Osaka University Graduate School of Medicine, Osaka, Japan.

[2] Department of Ophthalmology, Osaka University Graduate School of Medicine, Osaka, Japan.

[3] Topcon Research Institute, Tokyo, Japan.

Financial Disclosure(s):
The funding organization had no role in the design or conduct of this research.

Supported by the Ministry of Health, Labor and Welfare, Tokyo, Japan (Health Sciences Research grant no.: H19-sensory-001).

Tatsuo Yamaguchi, Naoki Nakazawa, and Toshifumi Mihashi are employees of Topcon.

Correspondence:
Takashi Fujikado, MD, Department of Applied Visual Science, Osaka University Graduate School of Medicine, 2-2 Yamadaoka, Suita, Osaka 565-0871, Japan. E-mail: fujikado@ophthal.med.osaka-u.ac.jp.

J Artif Organs (2009) 12:206–209
DOI 10.1007/s10047-009-0467-2

ORIGINAL ARTICLE

Hirokazu Sakaguchi, MD · Motohiro Kamei, MD
Takashi Fujikado, MD · Eiji Yonezawa,
Motoki Ozawa, MS · Carmen Cecilia-Gonzalez, MD
Orlando Ustariz-Gonzalez, MD
Hugo Quiroz-Mercado, MD · Yasuo Tano, MD

Artificial vision by direct optic nerve electrode (AV-DONE) implantation in a blind patient with retinitis pigmentosa

Abstract The purpose of this study was to evaluate the efficacy and safety of artificial vision by using a direct optic nerve electrode (AV-DONE) in a blind patient with retinitis pigmentosa (RP). This device, comprising three wire electrodes (0.05 mm in diameter), was implanted into the optic disc of a patient with RP with no light perception vision and the device was left implanted. Six months later, visual sensations were elicited by electrical stimulation through each electrode and the thresholds for the phosphene perception elicited by pulses of 0.25-ms duration/phase and a pulse frequency of 320 Hz were 30, 5, and 70 μA for each electrode. The phosphenes, which ranged in size from that of a match head to an apple, were round, oval, or linear, primarily yellow, and focally distributed. The area of the phosphenes changed when the electrical stimulation was supplied from different electrodes. No complications arose during the follow-up period. Localized visual sensations were produced in a blind patient with advanced RP, suggesting that our system could lead to the development of a useful visual prosthesis system.

Received: January 10, 2009 / Accepted: May 13, 2009

H. Sakaguchi (✉) · M. Kamei · Y. Tano
Department of Ophthalmology, Osaka University Medical School, 2-2 Yamadaoka, E-7, Suita, Osaka 565-0871, Japan
Tel. +81-6-6879-3456; Fax +81-6-6879-3458
e-mail: sakaguh@ophthal.med.osaka-u.ac.jp

T. Fujikado
Department of Applied Visual Science, Osaka University Medical School, Suita, Japan

E. Yonezawa · M. Ozawa
NIDEK Co., Ltd., Gamagori, Japan

C. Cecilia-Gonzalez · O. Ustariz-Gonzalez · H. Quiroz-Mercado[1]
Vitreo and Retina Service, Asociacion Para Evitar la Ceguera, Mexico City, Mexico

Present address:
[1] University of Colorado and Denver Health Medical Center, Denver, CO, USA

Key words Human · Optic nerve · Retinitis pigmentosa · Visual sensation · Visual prosthesis

Introduction

No treatment can restore vision to patients with retinitis pigmentosa (RP) once they have lost sight. In 1968, one group evaluated a visual prosthesis in a blind patient.[1] Dobelle et al.[2] reported in 1974 that a blind patient identified light using electrical stimulation from an electrode on the visual cortex, which leads to the realization that blind patients may recover vision. However, the cortical electrode and the intracranial surgery to implant it carry a risk of major complications. Many groups worldwide have suggested different approaches for restoring vision, with the retina or the optic nerve as new targets for stimulation.[3–15] Reportedly, 78% of the bipolar cells and 30% of the ganglion cells remain intact in the retinas of patients with advanced RP.[16] Therefore, it seems reasonable to target the remaining neural cells using electrical stimulation.

A group of researchers in Belgium implanted a spiral cuff electrode that supported four electrodes around the optic nerve of a blind patient with RP.[11,12] Whenever the pulse width, current intensity, the number, or the frequency of the stimulus train was changed, the patient perceived the corresponding phosphenes at different locations. Using these data, a map was constructed of the phosphenes that were stimulated, and an image was reproduced by selection of the corresponding phosphenes from the map. A volunteer with RP and no residual vision recognized letters with this system.[12]

Our group is also attempting to create visual prosthesis using a direct optic nerve electrode method.[17–19] We have tested electrical stimulation of the optic nerve with wire-type electrodes inserted transvitreously as an alternative to conventional visual prostheses. The efficacy and safety of this procedure have been reported in acute and long-term animal studies.[17–19] The purpose of the current study was to evaluate the usefulness and safety of our system during a preliminary clinical trial in a blind patient with RP.

Methods

Patient

The patient was a 35-year-old woman with RP with no light perception in the right eye and with light perception in the left eye. She had lost light perception from her right eye at least 4 years earlier. She had exotropia in her right eye. There were no other ocular diseases or systemic disorders that may have caused the visual loss. Approval from the Institutional Ethics Committee Board and informed consent from the patient were obtained for this research at Asociacion Para Evitar la Ceguera, Mexico City. This trial adhered to the tenets of the Declaration of Helsinki.

Electrode implantation

The surgery to implant the electrode was performed with the patient under general anesthesia. Phacoemulsification was performed and a silicone tube (Silascon, Kaneka Medix Corp. Tokyo, Japan) containing Parylene-coated platinum wires (each 0.05 mm in diameter) was sutured at the four scleral quadrants around the eyeball with a 5-0 suture. A small segment (0.5 mm) of the active tips of the wires were uncoated. After a standard three-port pars plana vitrectomy was performed, posterior vitreous detachment was confirmed. The wire bundle then was inserted into the scleral incision, which was 3.5 mm from the limbus. Three wire tips were inserted into the optic nerve using two vitreoretinal forceps. The tips were inserted within the optic disc area at a depth of 1.0–2.0 mm as far from the center as possible to avoid the vessels. The wires were inserted at the 12, 3, and, 9 o'clock positions. Another wire was left in the vitreous cavity as a reference electrode. After implantation, the wires around the eyeball were covered with Tenon and conjunctival tissue.

Before electrical stimulation, a peritomy was performed and the wires were uncovered. The end of each wire was connected to the stimulator. After the session, the wires were covered again with Tenon as well as conjunctival tissue and left in place for 6 months until the next session. The peritomy allowed access to the wires and connection to the stimulator for the second electrical stimulation session.

Electrical stimulation

Biphasic, cathodic-phase-first, electrical pulse trains of 1 s total duration were applied to the electrodes on two occasions: 1 day and 6 months postoperatively. The resulting phosphene perceptions were explored for threshold and localization in the visual field.

The duration of the stimulus pulses was 0.25 ms/phase and the frequency was 40 Hz, 160 Hz, or 320 Hz. The current was increased from 5 to 200 or 300 μA and then reduced from 200 or 300 down to 5 μA. No stimulation (0 μA) was applied at least once every ten stimulations to determine if the patient could differentiate electrically generated phosphenes from spontaneous phosphenes.

A beeping sound was issued in synchrony with each real or fake stimulation train. The patient was questioned about her phosphene perceptions, the clock position (1 to 12 o'clock), the distance from the center (central, mid, far), the color, and the size compared to a match head (a diameter of 3 mm), a pea (7 mm), a coin (20 mm), a ping-pong ball (40 mm), a baseball (70 mm), and an apple (100 mm), all viewed at arm's length. Everyday conversational words were used to ensure correct communication with the patient, such that the positions of the phosphenes were described in polar coordinates of the visual field.[20] The threshold of the phosphene perception was identified as the stimulation current when more than 50% of the tests were positive for perception.

Results

Electrode implantation and follow-up

No complications occurred intraoperatively or during the follow-up period. The wires remained functionally stable for at least 6 months (Fig. 1).

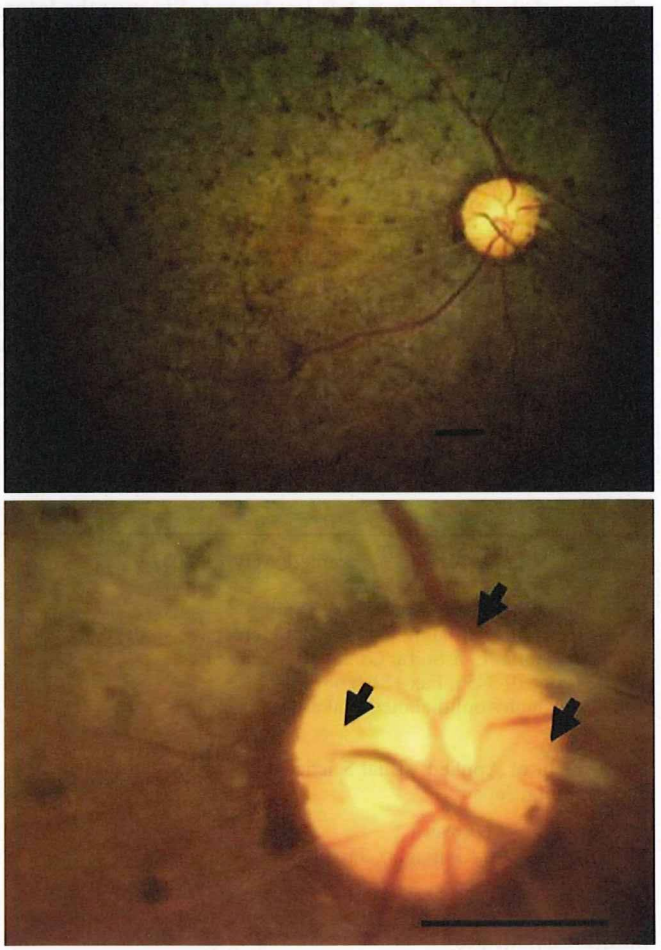

Fig. 1. The insertion of the platinum wire electrodes into the optic disc. *Upper*, three wire electrodes were inserted into the optic disc of the right eye, which had no light perception. *Lower*, the magnified image shows the electrode insertion sites (*arrows*). *Scale bar* 1.0 mm

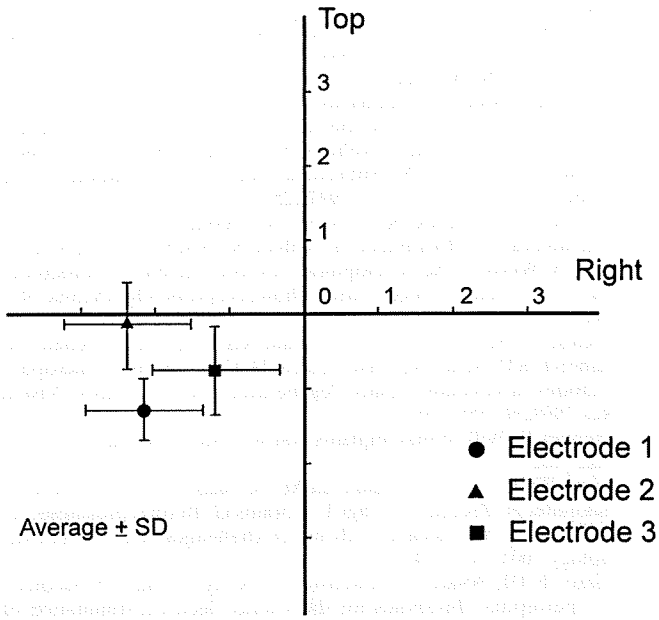

Fig. 2. The phosphenes generated by stimulation through each electrode were focally distributed in the visual field. The average central positions of the phosphenes clearly differ for each electrode

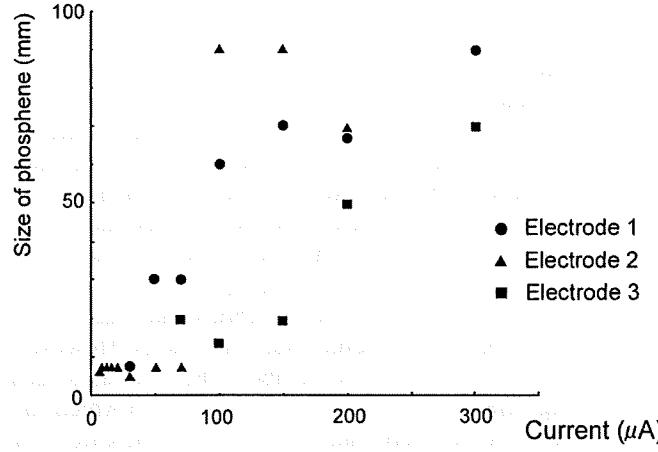

Fig. 3. The relationship between the size of the perceived phosphenes and the electrical stimulation. The sizes of the perceived phosphenes were significantly larger with higher electrical currents (Spearman rank order correlation: electrode 1 $r = 0.865$, $P < 0.05$; electrode 2 $r = 0.706$, $P < 0.05$; electrode 3 $r = 0.893$, $P < 0.05$)

Stimulation session

The patient identified electrically induced phosphenes from the first day after implantation. However, the data were unreliable because the patient could not distinguish clearly between artificial and spontaneous phosphenes, and she also seemed not to have understood the directions given to her. The entire stimulation session took about 3 h with the patient under topical anesthesia. Six months later, the identification of electrically induced phosphenes was reliable. The entire stimulation session took about 3 h using topical anesthesia.

The phosphenes generated by stimulation through each electrode were distributed focally in the visual field. The average phosphene center position differed for each electrode (Fig. 2). The size of the phosphenes was compared to objects ranging from a pea to an apple, from a match head to an apple, and from a pea to a baseball for electrodes 1, 2, and 3, respectively, all viewed at arm's length. The sizes of the perceived phosphenes were significantly larger with higher electrical currents (Spearman rank order correlation: electrode 1 $r = 0.865$, $P < 0.05$; electrode 2 $r = 0.706$, $P < 0.05$; electrode 3 $r = 0.893$, $P < 0.05$; Fig. 3). The patient described most of the 16 phosphenes from electrode 1 as yellow (14 yellow and 2 white) and all 20 and 10 phosphenes from electrodes 2 and 3, respectively, as yellow. The shapes of the phosphenes differed for each electrode. In total, 9 of the 16 phosphenes generated through electrode 1 were round and the other 7 were oval. Electrode 2 yielded 17 linear vertical phosphenes, 2 round phosphenes, and 1 linear horizontal phosphene. In total, 6 of the 10 phosphenes obtained with electrode 3 were linear horizontal in shape while 2 were linear vertical and the other 2 were round. No complications developed during the electrical stimulation session.

Discussion

We showed the feasibility of a new method to elicit artificial phosphene perceptions by electrical stimulation of optic nerve fibers with electrodes implanted through the optic disc in a blind patient with RP. A Belgian group also reported that a blind patient perceived phosphenes during electrical stimulation of the optic nerve fibers behind the eyeball.[11,12] These results clearly showed that the optic nerve fibers represent possible interface targets for visual prostheses.

The current study indicated that perceptions of a small phosphene, compared with a match head (about 23 arc min) or a pea (about 54 arc min) at arm's length, could be elicited by electrical stimulation of the optic nerve fibers. The sizes of the phosphenes significantly increased when stronger electrical currents were applied. This may result from recruitment of additional fibers around the electrode. The fact that small phosphenes were elicited suggests that a larger number of them could be induced independently using more electrodes in the optic disc, which would be an essential characteristic of our system. However, we should investigate further the effects of different electrical stimulation parameters. The shapes of the phosphenes differed for each electrode, which might indicate a combined effect of the local direction of the optic nerve fibers and the direction of insertion of the electrode wire.

The visual sensations were restricted to yellow in our trial. Humayun et al.[3] reported that four of five patients with light perception or no light perception with RP, retinal detachment, or age-related macular degeneration who could recognize localized phosphenes on electrical stimulation with an epiretinal electrode saw yellow or yellow–green

phosphenes, and one patient identified a white phosphene. Veraart et al.[11] showed that phosphenes produced by electrical stimulation with a cuff electrode around the optic nerve in a blind patient with RP were generally gold–yellow on the first day after surgery, and thereafter, blue, white, or plain yellow phosphenes were described, although the rates were not shown. The reason why the phosphenes were yellow in our trial is not well understood. This may result from electrical stimulation of the optic nerve or yellow may be the color associated with photoreceptor damage.

The current trial showed the possibility that our system may form the basis of a useful visual prosthesis. However, this system needs an active nerve fiber. Thus, diseases such as late-stage glaucoma and optic neuropathy, in which the nerve fibers are severely damaged, are not indicated for treatment with this system.

In the current study, the perceived position of the phosphenes in the visual field was determined by the electrode position in the optic nerve. With electrode contacts around the optic nerve periphery, a Belgian group reported that the position of the phosphenes in the visual field could be controlled by changing the stimulation train parameters including the pulse duration, current, frequency, and number.[11,12]

The current trial was limited by the absence of a transcutaneous transmission system. It was therefore impossible to draw a complete and accurate phosphene position map, which requires abundant data and consideration of the variability of subjective perceptions and a large number of parameters. A more advanced system is now under development that will allow us to complete this study in the near future.

To answer further questions about safety and efficacy, we need to observe more patients with this system, to perform more stimulation experiments to obtain more data, and to use a suitable system for energy and data supply to the electrodes.

Conclusion

Localized phosphene perceptions were elicited by stimulation of the optic disc electrode in a patient with advanced RP. Our data suggested that this system could lead to the development of a useful visual prosthesis system.

Acknowledgments This study was supported by a Grant-in-Aid for Scientific Research (A) from the Japan Society for the Promotion of Science, Japan, and a Health Sciences Research Grant from the Ministry of Health, Labor and Welfare, Japan. The authors thank J. Delbeke for helpful suggestions and critical reading of the manuscript.

References

1. Brindley GS, Lewin WS. The sensations produced by electrical stimulation of the visual cortex. J Physiol 1968;196:479–493
2. Dobelle WH, Mladejovsky MG, Girvin JP. Artificial vision for the blind: electrical stimulation of visual cortex offers hope for a functional prosthesis. Science 1974;183:440–444
3. Humayun MS, de Juan E Jr, Weiland JD, Dagnelie G, Katona S, Greenberg R, Suzuki S. Pattern electrical stimulation of the human retina. Vision Res 1999;39:2569–2576
4. Humayun MS, Weiland JD, Fujii GY, Greenberg R, Williamson R, Little J, Mech B, Cimmarusti V, Van Boemel G, Dagnelie G, de Juan E. Visual perception in a blind subject with a chronic microelectronic retinal prosthesis. Vision Res 2003;43:2573–2581
5. Chow AY, Chow VY. Subretinal electrical stimulation of the rabbit retina. Neurosci Lett 1997;225:13–16
6. Zrenner E, Miliczek KD, Gabel VP, Graf HG, Guenther E, Haemmerle H, Hoefflinger B, Kohler K, Nisch W, Schubert M, Stett A, Weiss S. The development of subretinal microphotodiodes for replacement of degenerated photoreceptors. Ophthalmic Res 1997;29:269–280
7. Zrenner E, Stett A, Weiss S, Aramant RB, Guenther E, Kohler K, Miliczek KD, Seiler MJ, Haemmerle H. Can subretinal microphotodiodes successfully replace degenerated photoreceptors? Vision Res 1999;39:2555–2567
8. Zrenner E. Will retinal implants restore vision? Science 2002;295: 1022–1025
9. Rizzo JF III, Wyatt J, Humayun M, de Juan E, Liu W, Chow A, Eckmiller R, Zrenner E, Yagi T, Abrams G. Retinal prosthesis: an encouraging first decade with major challenges ahead. Ophthalmology 2001;26:13–14
10. Rizzo JF III, Wyatt J, Loewenstein J, Kelly S, Shire D. Methods and perceptual thresholds for short-term electrical stimulation of human retina with microelectrode arrays. Invest Ophthalmol Vis Sci 2003;44:5355–5361
11. Veraart C, Raftopoulos C, Mortimer JT, Delbeke J, Pins D, Michaux G, Vanlierde A, Parrini S, Wanet-Defalque MC. Visual sensations produced by optic nerve stimulation using an implanted self-sizing spiral cuff electrode. Brain Res 1998;813:181–186
12. Veraart C, Wanet-Defalque MC, Gerard B, Valierde A, Delbeke J. Pattern recognition with the optic nerve visual prosthesis. Artif Organs 2003;27:996–1004
13. Sakaguchi H, Fujikado T, Fang X, Kanda H, Osanai M, Nakauchi K, Ikuno Y, Kamei M, Yagi T, Nishimura S, Ohji M, Yagi T, Tano Y. Transretinal electrical stimulation with a suprachoroidal multichannel electrode in rabbit eyes. Jpn J Ophthalmol 2004;48: 256–261
14. Nakauchi K, Fujikado T, Kanda H, Morimoto T, Choi JS, Ikuno Y, Sakaguchi H, Kamei M, Ohji M, Yagi T, Nishimura S, Sawai H, Fukuda Y, Tano Y. Transretinal electrical stimulation by an intrascleral multichannel electrode array in rabbit eyes. Graefes Arch Clin Exp Ophthalmol 2005;243:169–174
15. Fujikado T, Morimoto T, Kanda H, Kusaka S, Nakauchi K, Ozawa M, Matsushita K, Sakaguchi H, Ikuno Y, Kamei M, Tano Y. Evaluation of phosphenes elicited by extraocular stimulation in normals and by suprachoroidal-transretinal stimulation in patients with retinitis pigmentosa. Graefes Arch Clin Exp Ophthalmol 2007;245: 1411–1419
16. Santos A, Humayun MS, de Juan E Jr, Greenburg RJ, Marsh MJ, Klock IB, Milam AH. Preservation of the inner retina in retinitis pigmentosa. A morphometric analysis. Arch Ophthalmol 1997;115: 511–515
17. Sakaguchi H, Fujikado T, Kanda H, Osanai M, Fang X, Nakauchi K, Ikuno Y, Kamei M, Ohji M, Yagi T, Tano Y. Electrical stimulation with a needle-type electrode inserted into the optic nerve in rabbit eyes. Jpn J Ophthalmol 2004;48:552–557
18. Fang X, Sakaguchi H, Fujikado T, Osanai M, Kanda H, Ikuno Y, Kamei M, Ohji M, Gan D, Choi J, Yagi T, Tano Y. Direct stimulation of optic nerve by electrodes implanted in optic disc of rabbit eyes. Graefes Arch Clin Exp Ophthalmol 2005;243:49–56
19. Fang X, Sakaguchi H, Fujikado T, Osanai M, Ikuno Y, Kamei M, Ohji M, Yagi T, Tano Y. Electrophysiological and histological studies of chronically implanted intrapapillary microelectrodes in rabbit eyes. Graefes Arch Clin Exp Ophthalmol 2006;244: 364–375
20. Bishop PO, Kozak W, Vakkur GJ. Some quantitative aspects of the cat's eye: axis and plane of reference, visual field co-ordinates and optics. J Physiol 1962;163:466–502

Imaging of Titanium:Sapphire Laser Retinal Injury by Adaptive Optics Fundus Imaging and Fourier-Domain Optical Coherence Tomography

YOSHIYUKI KITAGUCHI, TAKASHI FUJIKADO, SHUNJI KUSAKA, TATSUO YAMAGUCHI, TOSHIFUMI MIHASHI, AND YASUO TANO

• PURPOSE: To examine and observe the subtle retinal injuries caused by a titanium:sapphire laser with a high-resolution adaptive optics (AO) fundus camera and with Fourier-domain optical coherence tomography (FD-OCT).

• DESIGN: Observational case series.

• METHODS: Four eyes of 2 individuals who experienced an accidental exposure to reflected light from a titanium: sapphire laser were examined. High-resolution retinal images were obtained with the AO fundus camera and by FD-OCT, and the images were compared with the findings obtained by standard clinical tests, including the Amsler test and fluorescein angiography (FA).

• RESULTS: The photoreceptor mosaic was absent in a localized area of the fovea in the images obtained by the AO fundus camera, and the photoreceptor outer segments (OS) were disrupted at the corresponding area in the FD-OCT images. The changes were detected not only in the symptomatic eye but also in the asymptomatic fellow eye in both patients. In 3 eyes, the geographic dark area in the AO image decreased during the follow-up examinations.

• CONCLUSIONS: Very small, localized photoreceptor disruptions can be detected in patients with minimal titanium:sapphire laser injury by cross-sectional imaging using OCT, but their extent was delineated more precisely by en face AO imaging. Because the area of the photoreceptor disruption is very small, especially in the nonsymptomatic fellow eye, it is strongly recommended that laser workers—even those without visual symptoms—be examined by FD-OCT, an AO camera, or both if they have not worn protective goggles while using a laser. (Am J Ophthalmol 2009;148:97–104. © 2009 by Elsevier Inc. All rights reserved.)

Accepted for publication Jan 21, 2009.

From the Department of Applied Visual Science, Osaka University Graduate School of Medicine (Y.K., T.F., S.K.); and the Department of Ophthalmology, Osaka University Graduate School of Medicine (Y.T.), Osaka, Japan; and the Topcon Research Institute (T.Y., T.M.), Tokyo, Japan.

Inquiries to Takashi Fujikado, Department of Applied Visual Science, Osaka University Graduate School of Medicine, 2-2 Yamadaoka, Suita, Osaka 565-0871, Japan; e-mail: fukikado@ophthal.med.osaka-u.ac.jp

ACCIDENTAL RETINAL LASER INJURIES ARE DIAGnosed when retinal damage is detected that is consistent with the visual deficits.[1] Intraretinal or subretinal hemorrhages, vitreous hemorrhages, macular edema, retinal pigmentation, and macular holes have been reported in many cases.[2] These alterations have been detected by conventional ophthalmoscopic examinations, including fluorescein angiography (FA) and optical coherence tomography (OCT). However, in cases of indirect exposure to scattered or reflected light or to long-duration exposures to a low-power laser beam, for example, a laser pointer, the retinal damage sometimes is undetectable by conventional ophthalmologic examinations despite the report of visual disturbances.[3]

With advances in retinal imaging, small focal changes in the retina can be detected. Fourier-domain OCT (FD-OCT) provides an axial resolution of approximately 3 μm compared with 10 μm with the standard OCT.[4–7] This resolution allows the identification of the external limiting membrane (first reflection line), the photoreceptor inner and outer segment junction (IS/OS; second line), the photoreceptor OS (between the second and third line), and the retinal pigment epithelium (RPE; fourth line).[4,7] This has enabled examiners to detect a lesion, for example, of the photoreceptor layer that cannot be detected by other examination methods. A disturbance of IS/OS junction has been reported in some retinal diseases, for example, postoperative retinal detachment, central serous chorioretinopathy, and retinal dystrophy, which cannot be seen ophthalmoscopically.[5,7,8–11] A macular microhole is difficult to detect ophthalmoscopically,[12] but can be detected reliably as a disruption of the outer retina or RPE layer by OCT[13] and as a disruption of the third line in the FD-OCT images.[14]

An adaptive optics (AO) fundus camera can obtain images with a transverse resolution of less than 2 μm, and the images of individual photoreceptors can be studied in living human eyes.[15–19] The origin of the high-reflectance cone mosaic in the AO fundus camera has been reported to be from both the IS/OS junction and the OS in normal retinas.[20] However, a recent study using AO-OCT reported that the cone mosaic was observed clearly at the level of the third bright line of the FD-OCT images, where the tips of the cone photoreceptor OS are enveloped by

0002-9394/09/$36.00
doi:10.1016/j.ajo.2009.01.019

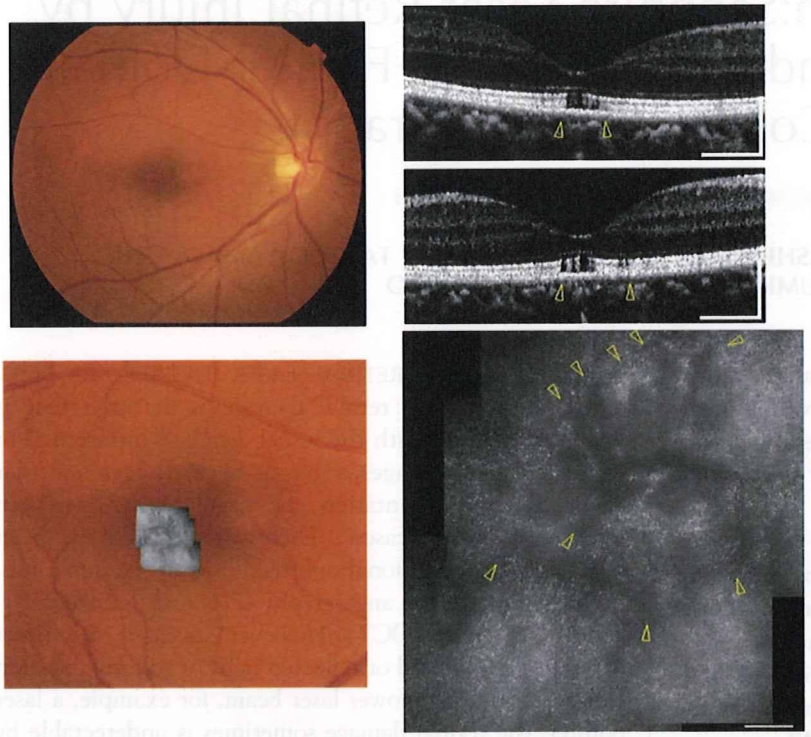

FIGURE 1. (Top left) Fundus photograph, (Top right [horizontal scan] and Middle right [vertical scan]) Fourier-domain optical coherence tomography (FD-OCT) images, and (Bottom left [low magnification] and Bottom right [high magnification]) adaptive optics (AO) images of the right eye of Patient 1 with titanium:sapphire retinal injury at the initial visit. The FD-OCT image shows a disruption of the photoreceptor inner segment and outer segment junction (IS/OS) and the OS (arrow head). The AO images show a geographic line-shaped dark area (arrowhead) above the fixation point. (Top right and Middle right) Horizontal bars represent 500 μm and vertical bars represent 200 μm. (Bottom right) Horizontal bar represents 100 μm.

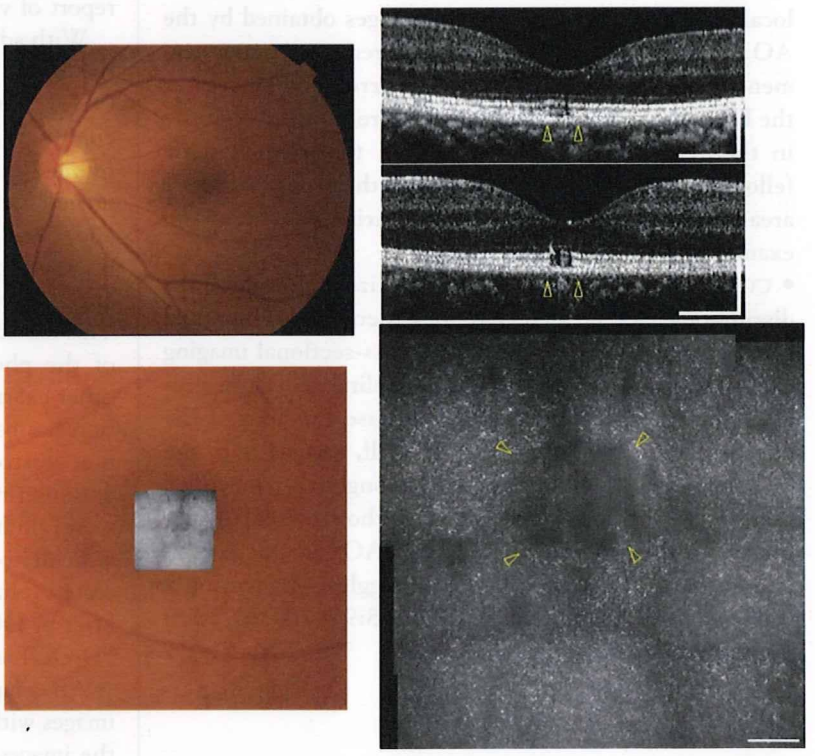

FIGURE 2. (Top left) Fundus photograph, (Top right [horizontal scan] and Middle right [vertical scan]) FD-OCT images, and (Bottom left [low magnification] and Bottom right [high magnification]) AO images of the left eye of Patient 1 with titanium:sapphire retinal injury at the initial visit. The FD-OCT image shows a disruption of the photoreceptor IS/OS and the OS (arrowhead). The AO images show a dark spotty area (arrowhead), and the area is smaller than that of right eye. (Top and Middle right) Horizontal bars represent 500 μm and vertical bars represent 200 μm. (Bottom right) Horizontal bar represents 100 μm.

the microvilli.[21] In our study of eyes with a macular microhole,[14] the OS may contribute more to the reflectance of the photoreceptor mosaic than the IS/OS junction in the AO images.

A reduction in the cone density in eyes with retinal dystrophy can be detected with an AO camera,[22,23] and a disruption of the third bright line of the FD-OCT images is reported to coincide with the dark areas in the AO camera images.[14]

Thus, the purpose of this study was to determine the cause of the visual disturbances reported by 2 patients who had worked with a titanium:sapphire laser. We show that the images obtained with the FD-OCT and AO both in depth and in the en face directions demonstrated retinal

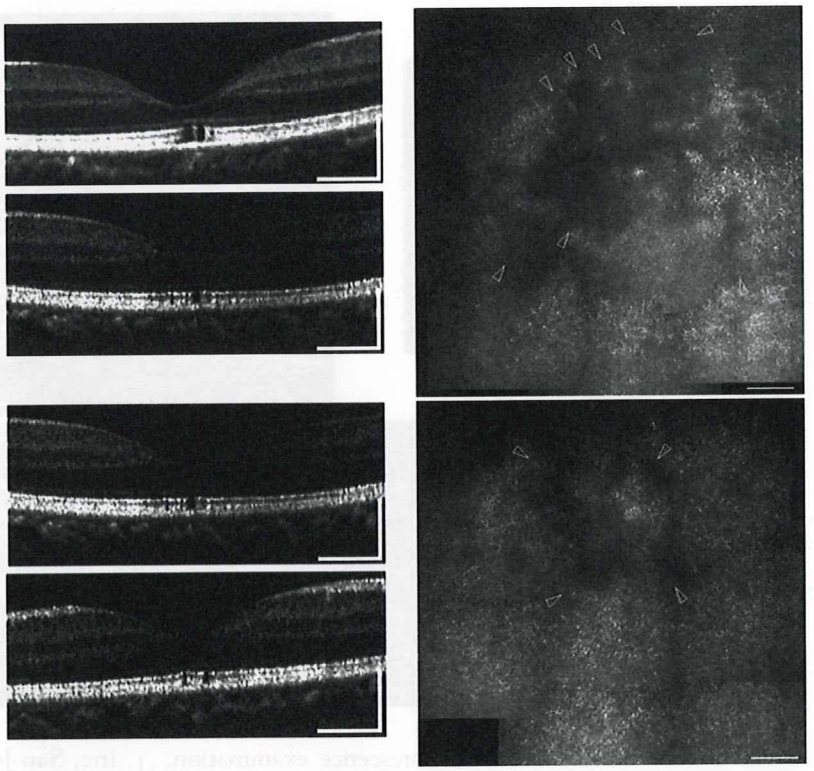

FIGURE 3. (Top left [horizontal scan] and second left [vertical scan]) FD-OCT images and (Top right) AO image of the right eye, and (Third left [horizontal scan] and Bottom left [vertical scan]) FD-OCT images (Bottom right) and AO image of the left eye of Patient 1 with titanium: sapphire retinal injury 6 months after the initial visit. The FD-OCT images are similar to that of the initial visit in both eyes. The AO image shows that the margin of line-shaped dark area is obscured in the right eye and that the dark spotty area has faded in the left eye. Horizontal bars in the left columns represent 500 μm, and vertical bars in the right columns represent 200 μm. Horizontal bar in the right column represents 100 μm. The arrowheads indicate the size of initial lesion.

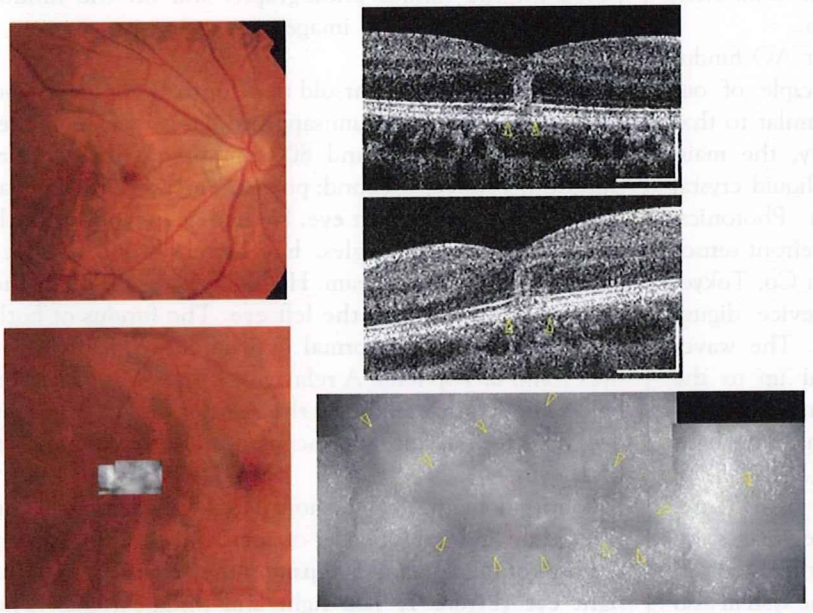

FIGURE 4. (Top Left) Fundus photograph, (Top right [horizontal scan] and Middle right [vertical scan]) FD-OCT images, and (Bottom left [low magnification] and Bottom right [high magnification]) AO images of the right eye of Patient 2 with titanium:sapphire retinal injury at the initial visit. FD-OCT image shows a penetrating lesion from the outer nuclear (ONL) layer to outer segment layer (OSL) in the fovea (arrowhead). The AO images show several spotty dark areas (arrowhead). (Top right and Middle right) Horizontal bars represent 500 μm and vertical bars represent 200 μm. (Bottom right) Horizontal bar represents 100 μm.

damage that was not visible by conventional ophthalmic instruments.

METHODS

• SUBJECTS: Two patients who reported visual disturbances after working with a titanium:sapphire laser beam were studied. The patients had visited the Osaka University Hospital between October 30, 2007 and June 13, 2008 and were followed up for more than 1 month. After the nature and possible consequences of the study were explained, written informed consent was obtained from the 2 patients.

• PROCEDURES: The 2 patients underwent a comprehensive ophthalmologic examination, including measurements of the best-corrected visual acuity (BCVA), Amsler chart testing, fundus photography, and slit-lamp biomicroscopy of the fundus. One patient underwent FA and the

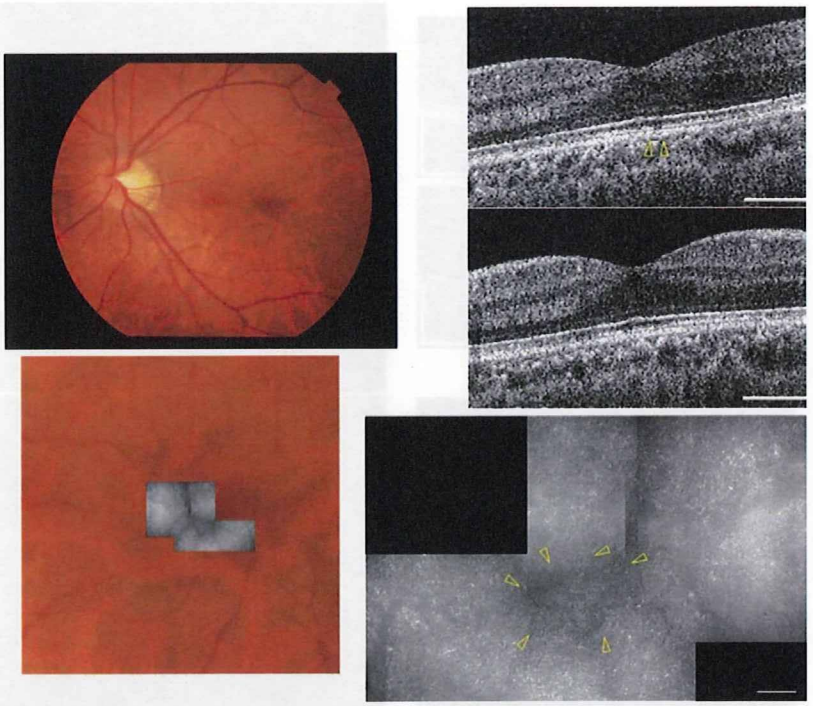

FIGURE 5. (Top left) Fundus photograph, (Top right [horizontal scan] and Middle right [vertical scan]) FD-OCT images, and (Bottom left [low magnification] and Bottom right [high magnification]) AO images of the left eye of Patient 2 with titanium:sapphire retinal injury at initial visit. The FD-OCT image shows a tiny OSL disturbance (arrowhead) on the horizontal scan. The AO images show a very small spotty dark area (arrowhead). (Top right and Middle right) Horizontal bars represent 500 μm and vertical bars represent 200 μm. (Bottom right) Horizontal bar represents 100 μm.

other underwent a fundus autofluorescence examination. They were also examined with the cube mode of FD-OCT (Cirrus OCT; Carl Zeiss Meditec, Dublin, California, USA) and a custom-built AO fundus camera.

A detailed description of the custom-built AO fundus camera has been published.[24,25] The principle of our flood-illumination AO fundus camera was similar to that reported by Roorda and Williams.[16] Briefly, the main components of the camera were a nematic liquid crystal phase modulator (X8267-12; Hamamatsu Photonics, Hamamatsu, Japan), a Hartmann-Shack wavefront sensor (28 × 28 lenslets, specially made by Topcon Co, Tokyo, Japan), and a scientific charge-coupled device digital camera (C9100-02; Hamamatsu Photonics). The wavefront sensor measured the ocular wavefront up to the eighth Zernike order, and the phase modulator compensated for the measured wavefront aberrations. The light source for the imaging was a laser diode (LLS-635-50; Moritex, Tokyo, Japan) with a wavelength of 635 nm. Because the light source was coherent, the images we obtained were different from those of an earlier study in which the light source was noncoherent.[16] The system also was equipped with coaxial, 8-degree wide viewing optics to identify the location and orientation of the highly magnified retinal images being examined.

Topical tropicamide (0.5%) and phenylephrine (0.5%) were used to dilate the pupil and to paralyze the ciliary muscle. The retina was illuminated by a laser diode (635-nm wavelength), and a retinal image was obtained with a shutter of 2 milliseconds with a 6-mm diameter exit pupil. The patient was instructed to fixate on a designated position on a target. Overlapping images were merged using Photoshop (Adobe Systems Inc, San Jose, California, USA). To identify the fovea, a montage of the AO images was made and superimposed on the fundus photographs and on the fundus projection of the OCT images.

• **PATIENT 1:** A 44-year-old male optical engineer who worked with a titanium:sapphire laser (pulse mode; wavelength, 400 nm and 800 nm; frequency, 1 kHz; duration, 100 femtosecond; power, 1 mJ) reported visual disturbances in his right eye. He had been working with the laser without goggles, but had not had a direct exposure to the laser beam. His BCVA was 20/50 in the right eye and 20/20 in the left eye. The fundus of both eyes appeared to be normal ophthalmoscopically (Figures 1 and 2, Top left). A relative scotoma was identified below the fixation point by the Amsler test in the right eye. The retinal autofluorescence image was normal in both eyes.

Fourier-domain OCT demonstrated a disruption of the IS/OS line and the OS layer of approximately 300 μm on the horizontal scan and 500 μm on the vertical scan of his right eye (Figure 1, Top right and Middle right). The external limiting membrane and RPE layer were intact. Interestingly, there was also a 200 × 200-μm disruption of the OS layer in his left eye (Figure 2, Top right and Middle right).

The AO image showed a very small dark area, that is, an absence of the cone mosaic, at the fovea just above the fixation point in both eyes. The shape of dark area was geographic, several line-shaped dark areas extended radially in the right eye, and a round dark area in the left eye was present (Figures 1 and 2, Bottom right). The area was larger in the right eye than in the left eye. The horizontal

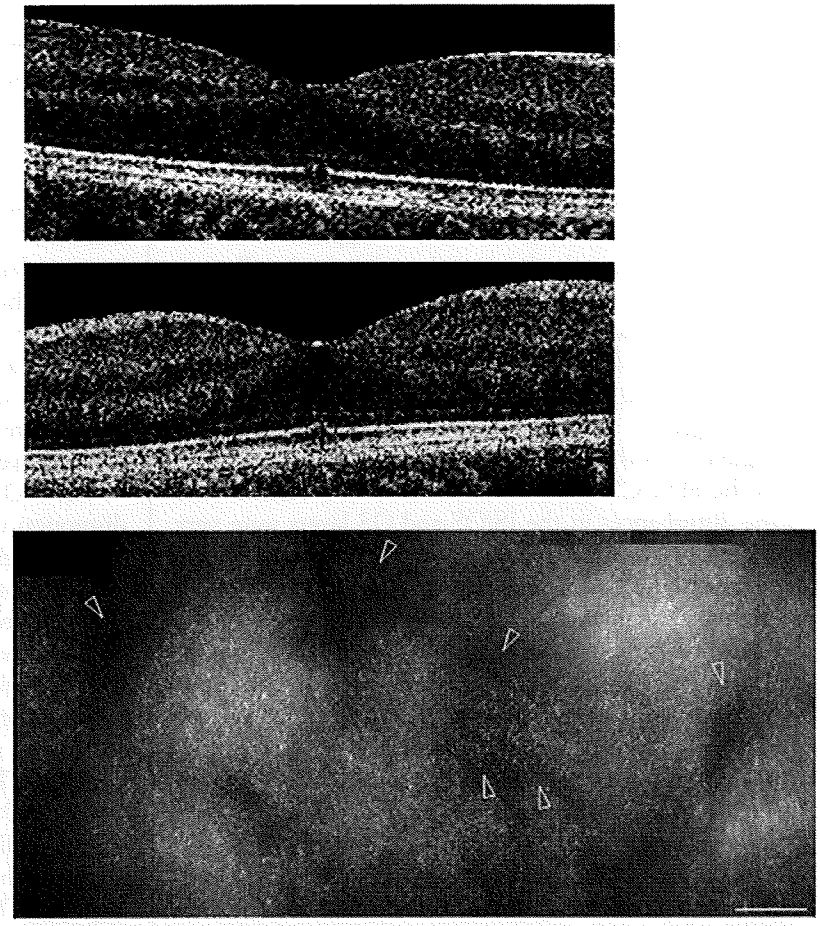

FIGURE 6. (Top [horizontal scan] and Middle [vertical scan]) FD-OCT image and (Bottom) AO image of the right eye of Patient 2 with titanium:sapphire retinal injury obtained 1 month after the initial visit. The FD-OCT image shows an almost intact ONL, and the size of disruption of the photoreceptor IS/OS junction and OS layer (arrowhead) is less than that at the initial visit. The AO images show that the area of the dark spots (arrowhead) also is reduced. (Top and Middle) Horizontal bars represent 500 μm and vertical bars represent 200 μm. (Bottom) Horizontal bar represents 100 μm.

and vertical sizes of the dark areas were 300 × 500 μm in the right eye and 200 × 200 μm in the left eye, and these sizes were comparable with those of the FD-OCT images of both eyes.

Six months after the first visit, his symptoms, the visual acuity (VA), and the area of IS/OS disruption in the FD-OCT (Figure 3, Top left, Second left, Third left, and Fourth left) had not changed in both eyes, but the margin of the line-shaped dark areas in the AO image was not well defined in the right eye, and the round dark area had faded in the left eye (Figure 3, Top right and Bottom right). The patient had not worked with the laser during this period.

• PATIENT 2: A 24-year-old male graduate student who worked in a chemistry laboratory using a titanium:sapphire laser (780 nm, 200-mW pulse mode). He had worked with a laser without wearing goggles and accidentally stared at the reflected laser beam from the wall of a cell during the alignment procedures the day before the first visit. He reported blurred vision in his right eye.

His BCVA was 20/25 in the right eye and 20/20 in the left eye. His fundus appeared to be normal without edema or retinal hemorrhage ophthalmoscopically (Figure 4, Top left). Amsler chart examination showed a localized relative scotoma around the fixation point. FA results were normal in both eyes.

Fourier-domain OCT demonstrated a penetrating lesion from the outer nuclear layer (ONL) to the OS layer in the fovea of the right eye (Figure 4, Top and Middle right). The area of disturbance in the IS/OS junction was approximately 200 μm on the horizontal scan and 300 μm on the vertical scan. There was a small OS layer disturbance (100 μm on the horizontal scan) in his left eye (Figure 5, Top right).

The AO image showed several spotty dark areas in the right eye ranging from approximately 800 μm horizontally and 400 μm vertically and a very small spot in the left eye (400 × 400 μm; Figures 4 and 5, Bottom right). The horizontal and vertical sizes of the dark area in the AO image were larger than the IS/OS or OS disturbances in those of FD-OCT scan in both eyes.

One month after the first visit, the subjective symptoms improved in the right eye and the area of relative scotoma was reduced in the Amsler chart. The VA in the right eye improved to 20/20. The penetrating lesion in the ONL in the FD-OCT scan could not be detected, and the size of the disruption of the IS/OS junction and the OS layers was reduced in the right eye (Figure 6, Top and Middle). The

area of the dark spots in the AO images was also reduced (Figure 6, Bottom).

RESULTS

BOTH OF THE PATIENTS EXPERIENCED AN EXPOSURE TO reflected light from a pulsed titanium:sapphire laser. Patient 1 did not note the bright reflected light, but Patient 2 looked at the bright reflected light. The fundus photographs had normal results in both eyes of both patients. The retinal autofluorescence image showed normal results in Patient 1, and the FA results were normal in Patient 2, which suggested that the disturbances of the RPE were negligible in both cases.

In the FD-OCT scans, the horizontal and vertical sizes of the disturbances in the IS/OS and OS layers were very restricted in both patients, and they coincided with the dark area of the AO image in both eyes of Patient 1, but were smaller than the dark area in the AO image of the right eye of Patient 2. The disturbances in the photoreceptors in the FD-OCT or AO images were observed not only in the symptomatic eye but also in the asymptomatic fellow eye in both patients.

In the right eye of Patient 1, the shape of dark area in AO had a geographic pattern in which several line-shaped dark areas were gathered radially, suggesting that the subclinical retinal injuries had been accumulating. During the follow-up, the margin of the dark areas in the AO image was obscured in Patient 1, and the penetrating injury in the nuclear layer disappeared with a reduction in the size of the IS/OS disruption in FD-OCT images and with a reduction of the area of dark spots in AO images in Patient 2.

DISCUSSION

THESE RESULTS INDICATE THAT MINIMAL RETINAL LASER damages, which are difficult or even impossible to detect with conventional ophthalmologic instruments, can be detected clearly by FD-OCT in depth or with an AO fundus camera in the en face direction. The AO camera enables an examination of the lateral extent of the defect, whereas the FD-OCT allows a cross-sectional examination of the photoreceptor disturbances in vivo. We have reported that disturbances of the photoreceptor layer in eyes with a macular microhole were imaged clearly by FD-OCT and the lateral extent of the lesion could be detected by a flood-illumination AO camera.[14]

The localized photoreceptor disruption caused by reflected light from the titanium:sapphire laser was identified by FD-OCT and AO imaging. To the best of our knowledge, this is the first report of selective photoreceptor damage resulting from titanium:sapphire laser that was identified and observed using FD-OCT and AO.

The photoreceptor damages detected in the OCT or AO images are reportedly related to visual disfunction in some retinal diseases.[5,26–28] Ojima and associates used microperimetry in eyes with resolved central serous chorioretinopathy and showed focal areas with reduced retinal function. These areas corresponded with a defect of the IS/OS line or irregularity of the RPE layer.[28] Choi and associates and Duncan and associates reported a decrease in cone density measured with an AO fundus camera and showed that the cone density was correlated with the amplitude of the multifocal electroretinogram.[23,29] In our patients, a disruption of the foveal photoreceptors observed in the FD-OCT and AO images were consistent with the relative scotoma in the Amsler test in the more affected eyes.

The AO image showed that the area of photoreceptor disruption was not round, but rather geographic (Figure 1, Bottom right). The complicated pattern of the area of photoreceptor loss may not be reconstructed from the data of the current FD-OCT, so the en face AO image was useful in evaluating the 2-dimensional area of the photoreceptor damage.

In the right eye of Patient 2, a lesion that extended from the inner retina to the outer retina was detected by FD-OCT. The horizontal size of the lesion was approximately 200 μm (approximately 1.0 degree), which was much smaller than the visual angle of metamorphopsia measured by the Amsler test (oval shape with 8 × 4 degrees). The visual angle of the metamorphopsia corresponded to the area of photoreceptor disruption measured by the AO fundus image. This discrepancy may be because the interval of the horizontal scan was 50 μm by FD-OCT and the maximal extent of the lesion could not be measured precisely.

In the 1-month follow-up of the right eye of Patient 2, the vision recovered to some extent with the disappearance of penetrating lesion in the ONL in the FD-OCT image and a fading of the dark areas in the AO image. The exact mechanism that led to the visual recovery is not clear, but the imaging data suggest that a reorganization of the photoreceptor cells might have occurred after the acute stages of foveal injury. Even in Patient 1, whose vision did not recover, the margin of the line-shaped dark geographic area in the AO image was obscured during the follow-up. Because the patient did not carry out laser experiments during this period, a reorganization of photoreceptor cells also might have occurred. Such reorganization may imply either a lateral displacement of adjacent photoreceptors or a regeneration of the OS of the same photoreceptors.

Fluorescein angiography or autofluorescence imaging demonstrated that the RPE was not damaged in the 2 patients. The reported cases of retinal injury by neodymium:yttrium–aluminum–garnet or titanium:sapphire laser were more severe, and a macular hole developed accompanied by changes in the RPE.[30–34] The pulse

duration of the titanium:sapphire laser is very short, in fact, hundreds of femtoseconds, so the mechanical effect of shock waves predominates over the thermal effect. Both of the patients received indirect reflected light from the laser, so the energy to the retina was less than the direct exposure to the laser beam. These factors may explain why the damages were confined to the photoreceptor layer.

In both patients, a disruption of the photoreceptors caused by reflected light from the laser was detected in both eyes by FD-OCT and with the AO fundus camera, although they had no visual symptoms in their less-affected fellow eye and no abnormal findings were detected with conventional ophthalmologic examinations. It has been reported that 8% of laser injuries are binocular.[2] These findings suggest that there may be more binocular cases than reported, and these can be detected best by FD-OCT or with the AO fundus camera.

Patient 1 did not have a direct exposure of the laser beam, but based on the pattern of the dark area in the image obtained by the AO fundus camera, we suggest that repeated indirect exposures by scattered and reflected laser light might have a cumulative effect on the retina. Although no symptoms were observed in his left eye, visual disturbances may appear in the future if the patient continues working without goggles and experiences repeated minimal exposures to the retinas.

Both of our patients did not wear goggles when they were working with the laser. Wearing protective goggles is required by law in many countries; however, many workers work without goggles because wearing goggles reduces the field of vision and the light intensity.[35] We suggest that others who work with lasers also may have retinal laser injury that can be detected only by FD-OCT or by the AO fundus camera, even those without visual symptoms. Therefore, it may be necessary to examine the eyes of optical engineers who have been involved in experiments with a laser without wearing goggles, even if they do not have visual symptoms. The ability of FD-OCT or AO fundus camera to detect a very restricted lesion in the fovea also may be applicable to other sources or forms of photic injury.

Two limitations of this study are the small number of patients and the short follow-up. Future studies with larger numbers of patients may be helpful to determine whether photoreceptor damage and inner retinal damage will be repaired in the natural course of the recovery process. Another limitation is the resolution limit of cone photoreceptors in the fovea. The AO fundus camera had a transverse resolution of less than 2 μm,[15] but the photoreceptors in the fovea are smaller than this resolution limit. Thus, it is difficult to evaluate quantitatively the disturbance of photoreceptor cells in the center of the fovea.

In conclusion, extremely localized photoreceptor disruptions can be detected in patients with minimal titanium: sapphire laser injury by FD-OCT in the depth direction and by AO imaging in the en face direction. The geographic dark area in the AO images in Patient 1 suggests that the subclinical laser damage is cumulative and eventually leads to visual symptoms. Because a very small area of photoreceptor disruption was observed even in the nonsymptomatic fellow eye in both patients, it is strongly recommended that laser workers or researchers even without visual symptoms be checked by FD-OCT, an AO fundus camera, or both if they have not worn protective goggles.

THIS STUDY WAS SUPPORTED BY HEALTH SCIENCES RESEARCH GRANTS NO. H19-SENSORY-001 FROM THE MINISTRY OF Health, Labor and Welfare, Tokyo, Japan. Drs Yamaguchi and Mihashi are employees of Topcon Co. Involved in design of study (T.F., S.K.); conduct of study (Y.K., T.Y.); analysis and interpretation of data (Y.K., T.F.); writing the article (Y.K., T.F.); critical revision of the article (T.M., Y.T.); and preparation, review, and approval of the manuscript (S.K.). The research protocol was approved by the Institutional Review Board of the Osaka University Medical School. The procedures performed conformed to the tenets of the Declaration of Helsinki.

REFERENCES

1. Mainster MA, Stuck BE, Brown J Jr. Assessment of alleged retinal laser injuries. Arch Ophthalmol 2004;122:1210–1217.
2. Barkana Y, Belkin M. Laser eye injuries. Surv Ophthalmol 2000;44:459–478.
3. Sethi CS, Grey RH, Hart CD. Laser pointers revisited: a survey of 14 patients attending casualty at the Bristol Eye Hospital. Br J Ophthalmol 1999;83:1164–1167.
4. Drexler W, Sattmann H, Hermann B, et al. Enhanced visualization of macular pathology with the use of ultra-high resolution optical coherence tomography. Arch Ophthalmol 2003;121:695–706.
5. Schocket LS, Witkin AJ, Fujimoto JG, et al. Ultra-high resolution optical coherence tomography in patients with decreased visual acuity after retinal detachment repair. Ophthalmology 2006;113:666–672.
6. Alam S, Zawadzki RJ, Choi S, et al. Clinical application of rapid serial Fourier-domain optical coherence tomography for macular imaging. Ophthalmology 2006;113:1425–1431.
7. Ojima Y, Hangai M, Sasahara M, et al. Three-dimensional imaging of the foveal photoreceptor layer in central serous chorioretinopathy using high-speed optical coherence tomography. Ophthalmology 2007;114:2197–2207.
8. Ergun E, Hermann B, Wirtitsch M, et al. Assessment of central visual function in Stargardt disease/fundus flavimaculatus with ultra-high resolution optical coherence tomography. Invest Ophthalmol Vis Sci 2005;46:310–316.
9. Wirtitsch MG, Ergun E, Hermann B, et al. Ultra-high resolution optical coherence tomography in macular dystrophy. Am J Ophthalmol 2005;140:976–983.
10. Piccolino FC, Longrais RR, Ravera G, et al. The foveal photoreceptor layer and visual acuity loss in central serous chorioretinopathy. Am J Ophthalmol 2005;139:87–99.

11. Iida T, Hagimura N, Sato T, et al. Evaluation of central serous chorioretinopathy with optical coherence tomography. Am J Ophthalmol 2000;129:16–20.
12. Cairns JD, McCombe MF. Microholes of the fovea centralis. Aust N Z J Ophthalmol 1988;16:75–79.
13. Zambarakji HJ, Schlottmann P, Tanner V, et al. Macular microholes: pathogenesis and natural history. Br J Ophthalmol 2005;89:189–193.
14. Kitaguchi Y, Fujikado T, Bessho K, et al. Adaptive optics fundus camera to examine localized changes in the photoreceptor layer of the fovea. Ophthalmology 2008;115:1771–1777.
15. Liang J, Williams DR, Miller DT. Supernormal vision and high resolution retinal imaging through adaptive optics. J Opt Soc Am A Opt Image Sci Vis 1997;14:2884–2892.
16. Roorda A, Williams DR. The arrangement of three cone classes in the living human eye. Nature 1999;397:520–522.
17. Roorda A, Williams DR. Optical fiber properties of individual human cones. J Vis 2002;2:404–412.
18. Roorda A, Romero BF, Donnelly WJ, et al. Adaptive optics scanning laser ophthalmoscopy. Opt Express 2002;10:405–412.
19. Pallikaris A, Williams DR, Hofer H, et al. The reflectance of single cones in the living human eye. Invest Ophthalmol Vis Sci 2003;44:4580–4592.
20. Pircher M, Baumann B, Gotzinger E, Hitzenberger CK. Retinal cone mosaic imaged with transverse scanning optical coherence tomography Optics Lett 2006;31:1821–1823.
21. Zawadzki RJ, Choi SS, Jones SM, et al. Adaptive optics-optical coherence tomography: optimizing visualization of microscopic retinal structures in three dimensions. J Opt Soc Am A Opt Image Sci Vis 2007;24:1373–1383.
22. Wolfing JI, Chung M, Carrol J, et al. High-resolution retinal imaging of cone-rod dystrophy. Ophthalmology 2006;113: 1014–1019.
23. Choi SS, Doble N, Hardy JL, et al. In vivo imaging of the photoreceptor mosaic in retinal dystrophies and correlations with visual function. Invest Ophthalmol Vis Sci 2006;47: 2080–2092.
24. Kitaguchi Y, Bessho K, Yamaguchi T, et al. In vivo measurements of cone photoreceptor spacing in myopic eyes from images obtained by adaptive optics fundus camera. Jpn J Ophthalmol 2007;51:456–461.
25. Yamaguchi T, Nakazawa N, Bessho K, et al. Adaptive optics fundus camera using a liquid crystal phase modulator. Opt Rev 2008;15:173–180.
26. Ergun E, Hermann B, Wirtitsch M, et al. Assessment of central visual function in Stargardt disease/fundus flavimaculatus with ultra-high resolution optical coherence tomography. Invest Ophthalmol Vis Sci 2005;46:310–316.
27. Piccolino FC, Longrais RR, Ravera G, et al. The foveal photoreceptor layer and visual acuity loss in central serous chorioretinopathy. Am J Ophthalmol 2005;139:87–99.
28. Ojima Y, Tsujikawa A, Hangai M, et al. Retinal sensitivity measured with the micro perimeter 1 after resolution of central serous chorioretinopathy. Am J Ophthalmol 2008; 146:77–84.
29. Duncan JL, Zhang Y, Gandhi J, et al. High-resolution imaging with adaptive optics in patients with inherited retinal degeneration. Invest Ophthalmol Vis Sci 2007;48:3283–3291.
30. Sasahara M, Noami S, Takahashi M, et al. Optical coherence tomographic observations before and after macular hole formation secondary to laser injury. Am J Ophthalmol 2003;136:1167–1170.
31. Nehemy M, Torqueti-Costa L, Magalhães EP, et al. Choroidal neovascularization after accidental macular damage by laser. Clin Exp Ophthalmol 2005;33:298–300.
32. Newman DK, Flanagan DW. Spontaneous closure of a macular hole secondary to an accidental laser injury. Br J Ophthalmol 2000;84:1075.
33. Sakaguchi H, Ohji M, Kubota A, et al. Amsler grid examination and optical coherence tomography of a macular hole caused by accidental Nd:YAG laser injury. Am J Ophthalmol 2000;130:355–356.
34. Sou R, Kusaka S, Ohji M, et al. Optical coherence tomographic evaluation of a surgically treated traumatic macular hole secondary to Nd:YAG laser injury. Am J Ophthalmol 2003;135:537–539.
35. Kamijo Y, Ozawa T. Accidental laser eye in Japan [in Japanese]. Jpn Rev Clin Ophthalmol 2003;97:95–100.